Processing and Application of Ceramics 12 [3] (2018) 248–256
https://doi.org/10.2298/PAC1803248T

Synthesis of novel hard/soft ferrite composites particles with improved magnetic properties and exchange coupling

Faezeh Tavakolinia[1], Mohammad Yousefi[1,*], Seyyed Salman Seyyed Afghahi[2], Saeid Baghshahi[3], Susan Samadi[4]

[1]*Department of Chemistry, Science and Research Branch, Islamic Azad University, Tehran, Iran*
[2]*Department of Engineering, Imam Hossein University, Tehran, Iran*
[3]*Department of Materials Engineering, Faculty of Engineering, Imam Khomeini International University, Qazvin, Iran*
[4]*Department of Chemistry, Yadegar-e-Imam Khomeini (RAH), Shahre Rey Branch, Islamic Azad University, Tehran, Iran*

Received 21 February 2018; Received in revised form 18 June 2018; Accepted 14 August 2018

Abstract

$SrFe_{12}O_{19}/Zn_{0.4}Co_{0.2}Ni_{0.4}Fe_2O_4$ hard/soft ferrite composite particles with 20, 40, 60 and 80 wt.% of soft phase were prepared by one-pot sol-gel auto-combustion and physical mixing methods. Fourier transform infrared spectroscopy (FTIR), X-ray diffraction (XRD), field emission scanning electron microscope (FESEM) and vibrating sample magnetometer (VSM) were used to characterize the structural and magnetic properties of the samples. XRD spectrum revealed the formation of mixed ferrite phases in the composite particles. The hysteresis loops of the samples showed the presence of exchange coupling between the hard and soft ferrites. The composite particles with 20 and 60 wt.% of the soft phase demonstrated the highest M_r/M_s ratio, i.e. 0.29 and 0.28, respectively. In addition, the highest M_s, M_r and H_c were achieved in the composite particles with 40, 60 and 20 wt.% of the soft phase, respectively. Compared to the physical mixing method (PM), the composite particles prepared by the sol-gel auto-combustion method (OP) demonstrated better magnetic properties. The exchange coupling interaction between the hard and soft ferrite phases was similar in both methods. These composite particles exhibited magnetically single phase behaviour, however, the saturation magnetization was lower in the physical mixing pared to that of the one-pot method.

Keywords: *sol-gel auto-combustion, physical mixing, hard/soft composite ferrites, magnetic properties, exchange coupling*

I. Introduction

Magnetic composites are being used as magnetic fluids, microwave devices, biomedicines and permanent magnets in various applications [1]. Composite with hard ($SrFe_{12}O_{19}$) and soft ($Zn_{0.4}Co_{0.2}Ni_{0.4}Fe_2O_4$) phases can improve the magnetic properties because of the high exchange coupling of both phases. Consequently, with high exchange coupling between hard and soft phases, the high saturation magnetization of the soft phase and high coercivity of the hard phase can increase all magnetic properties rather than hard and soft phase itself [2]. Ferrite composites composed of spinel soft and hard ferrites are good candidates for advanced permanent magnets, because of their low cost, excellent corrosion resistance, relatively high Curie temperature and high electrical resistivity [3].

The hard/soft ferrite composites have been synthesized with good exchange spring interaction between two phases. Hard/soft composite powders such as $BaFe_{12}O_{19}/Mn_{0.2}Ni_{0.4}Zn_{0.4}Fe_2O_4$ [4], $BaFe_{12}O_{19}/NiFe_2O_4$ [5,6], $BaFe_{12}O_{19}/Ni_{0.65}Zn_{0.35}Fe_2O_4$ [7], $Co_{0.6}Zn_{0.4}Fe_2O_4/SrFe_{10.5}O_{16.75}$ [8], $SrFe_{12}O_{19}/Ni_{0.7}Zn_{0.3}Fe_2O_4$ [9], $SrFe_{10}Al_2O_{19}/Co_{0.8}Ni_{0.2}Fe_2O_4$ [10], $BaFe_{12}O_{19}/Ni_{0.5}Zn_{0.5}Fe_2O_4$ [11], $SrFe_{12}O_{19}/Ni_{0.5}Zn_{0.5}Fe_2O_4$ [12], $BaFe_{12}O_{19}/Y_3Fe_5O_{12}$ [13], $BaFe_{12}O_{19}/Fe_3O_4$ [14] and $BaFe_{12}O_{19}$-

*Corresponding authors: tel: +98 912 525 2435,
e-mail: *myousefi50@hotmail.com*

$Ni_{0.5}Zn_{0.5}Fe_2O_4$ [15] were prepared, but they could not reach the aim of intresting high exchange coupling between hard/soft ferrite nanocomposites [16]. Hard hexagonal and soft spinel ferrites with high corrosion resistance, good electrical resistivity and cost-effective materials can be used as a permanent magnet [5,6,12,17–22].

In the present research, the ferrite composite particles of $SrFe_{12}O_{19}$ as a hard phase and $Zn_{0.4}Co_{0.2}Ni_{0.4}Fe_2O_4$ as a soft phase were synthesized to obtain the high exchange coupling. $SrFe_{12}O_{19}$ is a hexagonal ferrite that has the highest coercivity among the other similar ferrites. $CoFe_2O_4$ has high saturation magnetization (M_s ~ 80 emu/g) [22], and this value could be changed by Ni and Zn doping. $SrFe_{12}O_{19}/Zn_{0.4}Co_{0.2}Ni_{0.4}Fe_2O_4$ hard/soft composite ferrites with various amount of the soft phase (20, 40, 60 and 80 wt.%) have been synthesized by the one-pot sol-gel auto-combustion and physical mixing methods to investigate exchange coupling behaviour.

II. Experimental

2.1. Sample preparation

In the present work, $SrFe_{12}O_{19}/Zn_{0.4}Co_{0.2}Ni_{0.4}Fe_2O_4$ hard/soft ferrite composite particles with 20, 40, 60 and 80 wt.% of soft phase were prepared by two different processing methods: i) one-pot sol-gel auto-combustion and ii) physical mixing. Iron nitrate nonahydrate ($Fe(NO_3)_3 \cdot 9\,H_2O$), strontium nitrate ($Sr(NO_3)_2$), zinc chloride ($ZnCl_2$), cobalt nitrate hexahydrate ($Co(NO_3)_2 \cdot 6\,H_2O$), nickel nitrate hexahydrate ($Ni(NO_3)_3 \cdot 6\,H_2O$) and citric acid ($C_6H_8O_7 \cdot H_2O$) (all from Merck) were used as precursors.

In one-pot sol-gel auto-combustion method, the stoichiometric amounts of Sr and Fe nitrates were dissolved in deionized water at 80 °C to get a brown solution. Then citric acid was added to the solution, with the molar ratio of metal ions to citric acid of 1 : 1.5. In another beaker, stoichiometric amounts of $Fe(NO_3)_3 \cdot 9\,H_2O$, $Co(NO_3)_2 \cdot 6\,H_2O$, $Ni(NO_3)_3 \cdot 6\,H_2O$, $ZnCl_2$ and citric acid were mixed and dissolved in deionized water. After obtaining a light brown clear solution, the solution was added to the first beaker containing strontium hexaferrite salts. The molar ratio of soft metallic ions to citric acid was 1 : 1. After 2 h, ammonia solution was added dropwise to adjust pH at 7 and the mixed solution was heated at 120 °C. The solution became a viscous gel while evaporating. Then gel ignited in the microwave oven device and the black-coloured powder was prepared. The powders were calcined at 500 °C for 5 h and then at 1200 °C for 2 h to form $SrFe_{12}O_{19}/Zn_{0.4}Co_{0.2}Ni_{0.4}Fe_2O_4$ composite particles.

In physical mixing method, $SrFe_{12}O_{19}$ and

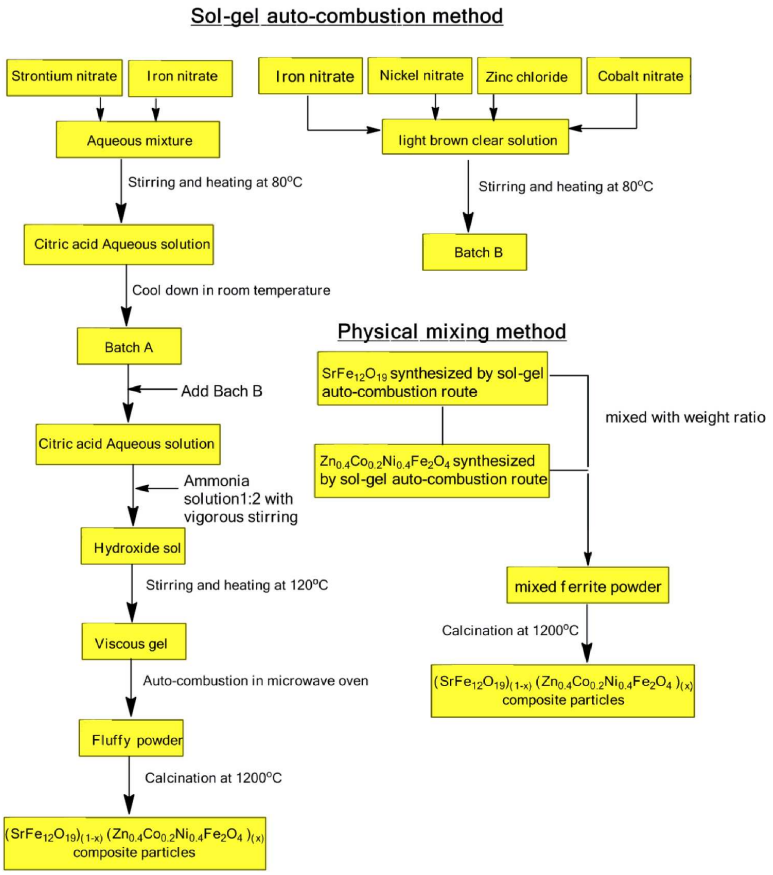

Figure 1. Synthesis procedure of $SrFe_{12}O_{19}/Zn_{0.4}Co_{0.2}Ni_{0.4}Fe_2O_4$ composites by sol-gel auto-combustion and physical mixing methods

$Zn_{0.4}Co_{0.2}Ni_{0.4}Fe_2O_4$ were synthesized separately by the sol-gel auto combustion method and then mixed with stoichiometric amount physically. The prepared samples were calcined at 1200 °C for 2 h (Fig. 1).

2.2. Characterization

X-ray diffraction measurements (XRD) were performed using a diffractometer (PW-1730, The Netherlands) with Cu Kα (1.54Å) radiation operated at 40 kV and 30 mA The morphology and composition of the composites were investigated by field emission scanning electron microscope (FE-SEM; TESCAN; Model MIRA3) and energy-dispersive spectroscopy spectrometer with 15 kV voltage. FTIR spectra were obtained by Fourier transform infrared spectrometer (NEXUS870). A vibrating sample magnetometer (VSM; ZVK, R&S) was used to measure the magnetic properties of the powders.

III. Results and discussion

3.1. Structural characterization - XRD analysis

XRD patterns of $SrFe_{12}O_{19}/Zn_{0.4}Co_{0.2}Ni_{0.4}Fe_2O_4$ composite particles prepared by one-pot and physical mixing methods (calcined at 1200 °C) are presented in Figs. 2a and 2b, respectively. There are only XRD peaks of the hard $SrFe_{12}O_{19}$ phase (JCPDS card No. 01-084-1531) and soft $Zn_{0.4}Co_{0.2}Ni_{0.4}Fe_2O_4$ phase (JCPDS card No. 01-087-2336), without any impurity peak, such as NiO, ZnO, $SrFe_2O_4$ or α-Fe_2O_3. Due to the fact that homogeneity of hard and soft phase is related to the synthesis method, the intensity of all peaks changes.

Table 1. Average crystallite size of $(SrFe_{12}O_{19})_{1-x}(Zn_{0.4}Co_{0.2}Ni_{0.4}Fe_2O_4)_x$ (x = 0.2, 0.4, 0.6, 0.8) composite powders prepared by one-pot sol-gel auto-combustion method and calcined at 1200 °C

Sample	Crystallite size [nm]	
	* (114) plane	# (311) plane
Pure soft	–	214
80% soft	83	34
60% soft	78	80
40% soft	53	58
20% soft	64	47
Pure hard	71	–

* For $SrFe_{12}O_{19}$

\# For $Zn_{0.4}Co_{0.2}Ni_{0.4}Fe_2O_4$

Based on the Scherrer's equation [23] and XRD 114 and 311 peaks of $SrFe_{12}O_{19}$ and $Zn_{0.4}Co_{0.2}Ni_{0.4}Fe_2O_4$ phases, the average crystallite sizes were calculated to be about 71 nm and 214 nm, respectively (Table 1). By increasing the amount of the soft phase, the average crystallite size is reduced to 69 nm and 53 nm for hard and soft phases, respectively. Cobalt-nickel-zinc ferrite inhibits the growth of strontium ferrite and improves the growth of soft phase rather than hard phase [10].

3.2. Structural characterization - FTIR analysis

Figure 3 shows the IR spectra of the $SrFe_{12}O_{19}/Zn_{0.4}Co_{0.2}Ni_{0.4}Fe_2O_4$ composite ferrites prepared by one-pot and physical mixing method. The spectra show absorption peaks at 438, 545, 596, 1128, 1633 and 2355 cm^{-1}. The bands around 570–600 and 438 cm^{-1} correspond to the characteristic bonds of $(SrFe_{12}O_{19})_{1-x}(Zn_{0.4}Co_{0.2}Ni_{0.4}Fe_2O_4)_x$ (x = 0.2, 0.4,

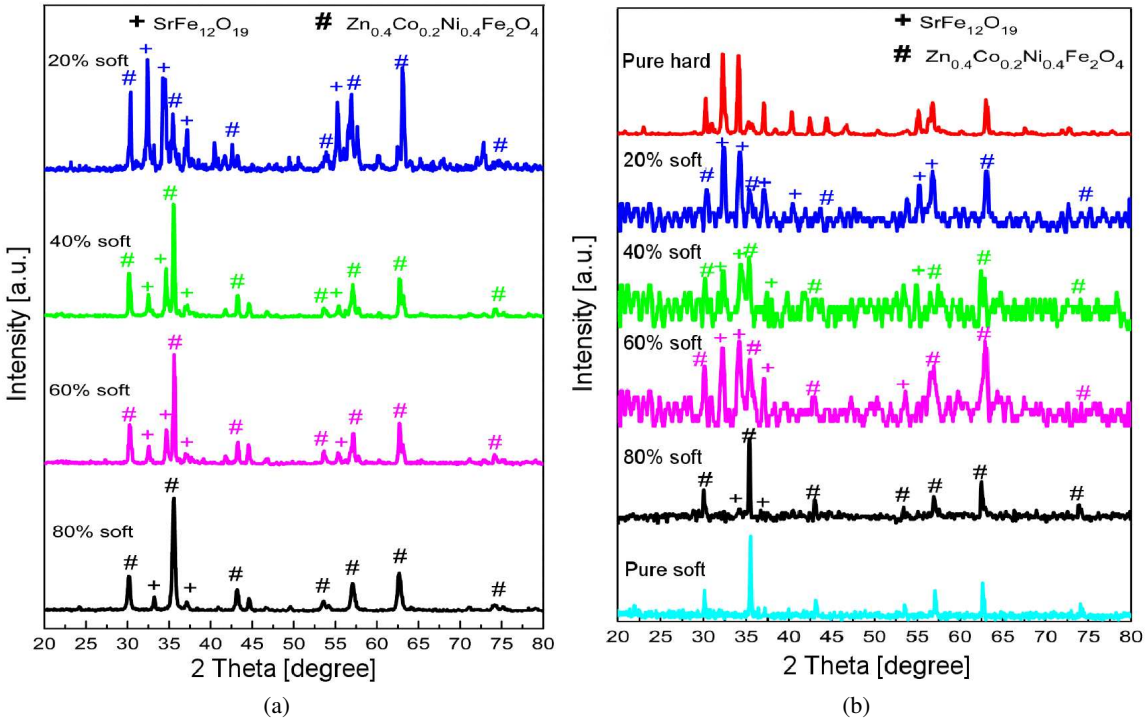

Figure 2. XRD patterns of $(SrFe_{12}O_{19})_{1-x}(Zn_{0.4}Co_{0.2}Ni_{0.4}Fe_2O_4)_x$ (x = 0.2, 0.4, 0.6, 0.8) composites prepared by: a) one-pot sol-gel auto-combustion route and b) physical mixing method

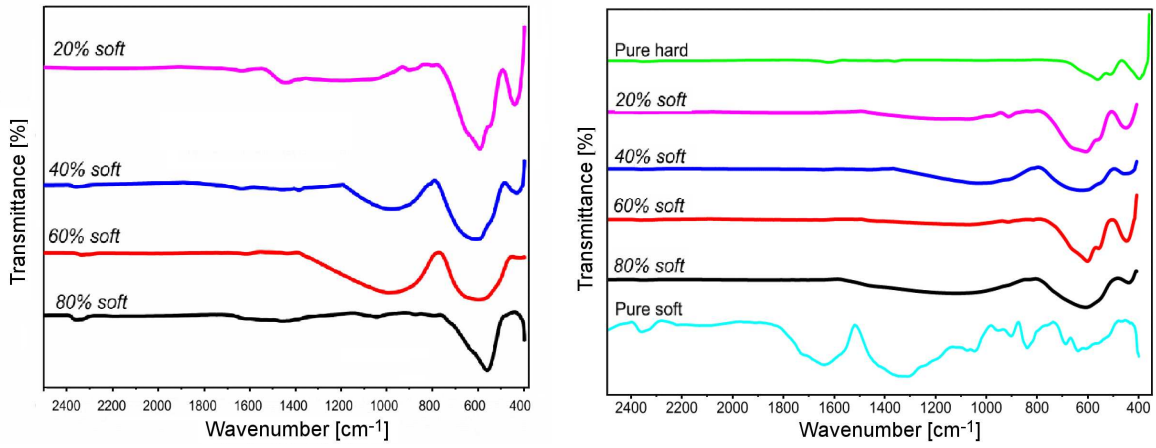

Figure 3. FT-IR spectra of $SrFe_{12}O_{19}/Zn_{0.4}Co_{0.2}Ni_{0.4}Fe_2O_4$ composites prepared by: a) physical mixing and b) one-pot method with various weight percentages of soft phase in the composite

0.6, 0.8) representing stretching vibration of iron and strontium bonds with oxygen. These are metal-oxide bonds in the strontium ferrite crystal lattice which reveal the formation of strontium ferrite. The bands at 1040 and 1128 cm^{-1} are related to the C–N bond formation during the synthesis process of strontium ferrite composites The band at 1625 cm^{-1} is related to asymmetric stretching of carbonyl groups (C=O). Also, the bands around 2350 cm^{-1} confirm the presence of carbonyl groups. The FTIR spectra of these compounds suggest that the hydroxyl stretching vibration of iron and strontium bonds with oxygen. In the FTIR spectra of all samples within the range from 800 to 400 cm^{-1}, the typical metal-oxygen absorption bonds confirm the formation of the hexagonal structure of strontium ferrite [21,24,25].

3.3. Structural characterization - FE-SEM results

The pure $SrFe_{12}O_{19}$ and $Zn_{0.4}Co_{0.2}Ni_{0.4}Fe_2O_4$ are presented in Figs. 4a and 4b, respectively. It can be seen from Fig. 4a that the pure hard phase calcined at 1200 °C has hexagonal platelet-like morphology. Figures 5a-h show FESEM micrographs of the hard/soft composites calcined at 1200 °C. The morphology of $Zn_{0.4}Co_{0.2}Ni_{0.4}Fe_2O_4$ particles is roughly spherical in shape. During one-step auto combustion process, ignition causes generation of huge amounts of gases that are released and highly porous nanoparticles are formed initially, but later only a few of them remain which grow in size at the cost of smaller ones. The larger grains correspond to the $SrFe_{12}O_{19}$, while smaller ones represent the $Zn_{0.4}Co_{0.2}Ni_{0.4}Fe_2O_4$ phase. Microstructure of the pure $SrFe_{12}O_{19}$ (Fig. 4a) shows large elongated grains with submicrometer size. $Zn_{0.4}Co_{0.2}Ni_{0.4}Fe_2O_4$ grains (Fig. 4b) are nearly spherical in shape with an average size of ~2 μm.

Comparing the microstructural features of the physically mixed samples (Figs. 5b,d,f h) with the ones from one-pot (Figs. 5a,c,e,g), it is obvious that the composite particles synthesized by one-pot method possess better homogeneous mixing of $Zn_{0.4}Co_{0.2}Ni_{0.4}Fe_2O_4$ and $SrFe_{12}O_{19}$ phase than the composite particles prepared by physical mixing method. This shows that the processing method plays an important role in defining the microstructure of composite. In addition, it is known that magnetic particles could induce their agglomeration and, thus, contribute to microstructural changes [25]. This difference in the microstructure of the samples may

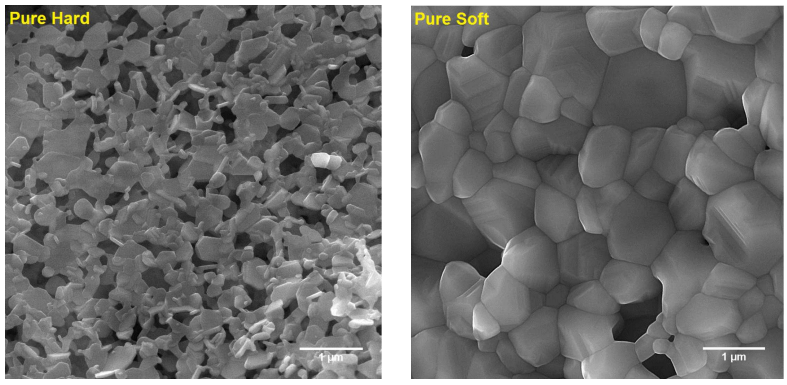

Figure 4. FESEM micrographs of $SrFe_{12}O_{19}$ and $Zn_{0.4}Co_{0.2}Ni_{0.4}Fe_2O_4$ samples prepared by one-pot sol-gel auto-combustion route

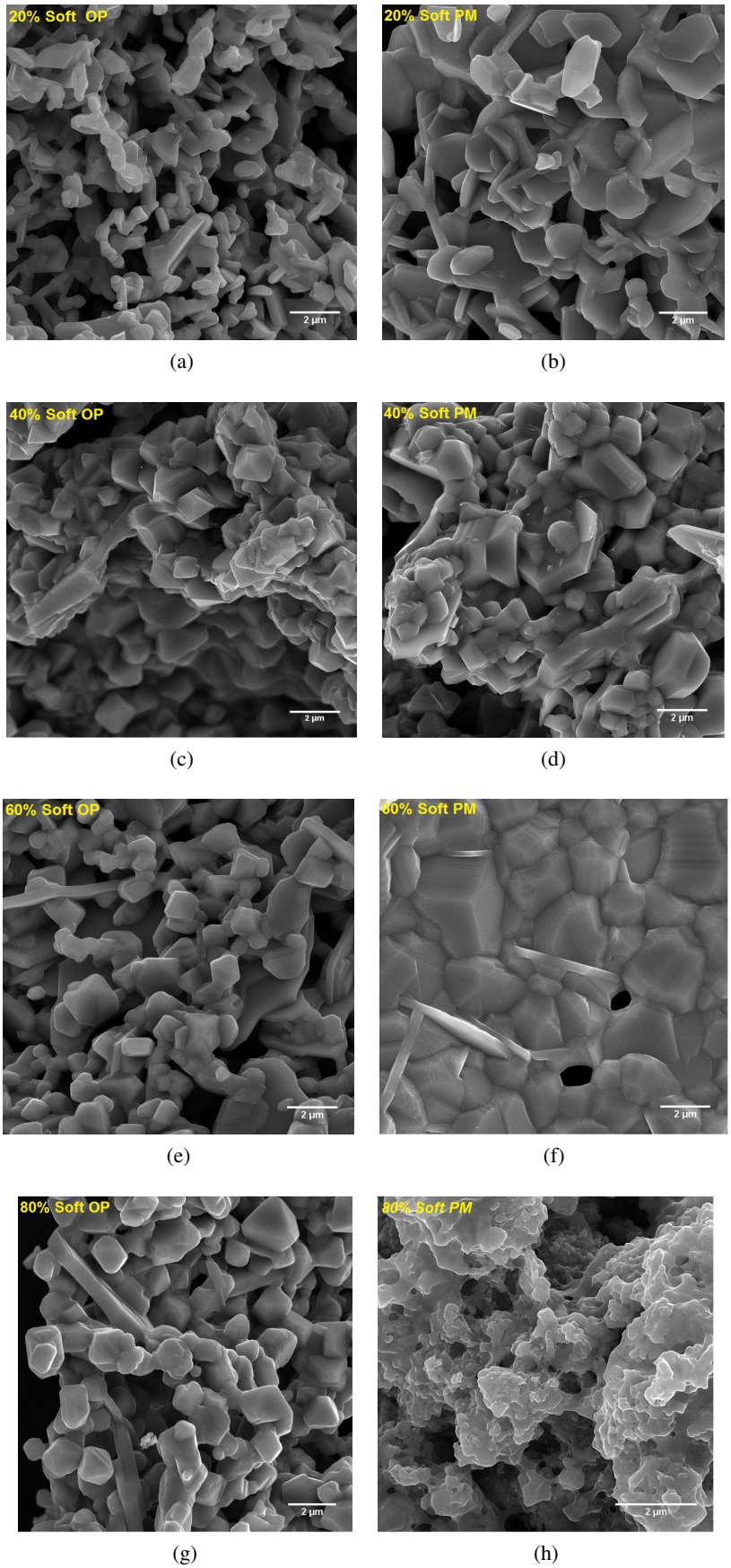

Figure 5. FESEM micrographs of $(SrFe_{12}O_{19})_{1-x}(Zn_{0.4}Co_{0.2}Ni_{0.4}Fe_2O_4)_x$ (x = 0.2, 0.4, 0.6, 0.8) composites prepared by one-pot and physical mixing method

Table 2. EDX element composition of $(SrFe_{12}O_{19})_{0.8}(Zn_{0.4}Co_{0.2}Ni_{0.4}Fe_2O_4)_{0.2}$ and $(SrFe_{12}O_{19})_{0.2}(Zn_{0.4}Co_{0.2}Ni_{0.4}Fe_2O_4)_{0.8}$ composites prepared by one-pot method

Sample	Fe	O	Ni	Zn	Co	Sr
80% soft	45.3	21	12	6.4	4.9	1.5
20% soft	64.6	23.5	2.2	3.2	1.1	5.5

play an important role in the magnetic and microwave absorption properties of the composites.

EDX analysis (Table 2) of the calcined composite particles indicated the presence of all the elements (e.g. Co, Ni, Zn, Fe, Sr, and O). EDX analysis showed that in the hard/soft composites, there was a good compromise with chemical stoichiometry.

The range of the exchange-coupling interaction between the grains of hard and soft magnetic phases, i.e., the exchange length, L_{ex}, can be expressed as [20,24,26]:

$$L_{ex} = \frac{A^2}{K^2 D^3} \tag{1}$$

where A and K denote the exchange stiffness and the mean amplitude of the random effective anisotropy constant, respectively, and D is the diameter of the grain. So, larger grain size reduces the exchange length and consequently the coupled regions.

3.4. Magnetic properties

Room temperature magnetic loops for the pure $SrFe_{12}O_{19}$ and $Zn_{0.4}Co_{0.2}Ni_{0.4}Fe_2O_4$ samples calcined at 1200 °C are given in Fig. 6. H_c = 5813 Oe, M_s = 46 emu/g and M_r = 26 emu/g were measured for $SrFe_{12}O_{19}$ powder. The high H_c value confirms that $SrFe_{12}O_{19}$ belongs to the hard magnetic materials. The saturation magnetization and coercivity of $Zn_{0.4}Co_{0.2}Ni_{0.4}Fe_2O_4$ are 67 emu/g and 64.7 Oe, respectively, confirming that $Zn_{0.4}Co_{0.2}Ni_{0.4}Fe_2O_4$ belongs to the soft magnetic materials.

Room temperature magnetic loops for the composite samples calcined at 1200 °C are given in Fig. 7. The *M-H* behaviour of the composite particles prepared by one-pot and physical mixing method shows a smooth curve without any step, meaning that the spinel and magnetoplumbite phase exchanged coupled with each other [27]. The magnetization and demagnetization force have single ferrimagnetic property, because of the external magnetic force and soft magnetic moments rotate along with the hard phase. The difference in the demagnetization behaviour is the interplay of three types of spin interactions in the composite particles, i.e. between soft/soft phase, hard/hard phase and hard/soft phases. The interfacial interaction between the hard and soft phases should be dominant for exchange couple systems. Also, the grain size of the soft phase should be smaller than the domain wall width of the hard phase [10,24]. The hard ferrite possesses a high magnetocrystalline anisotropy energy compared to the soft ferrite.

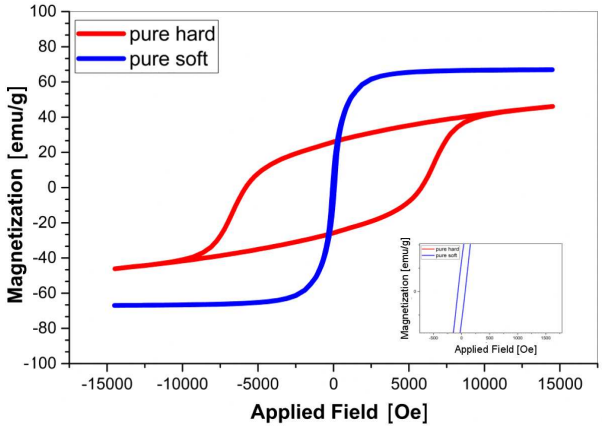

Figure 6. Hysteresis loops of $SrFe_{12}O_{19}$ and $Zn_{0.4}Co_{0.2}Ni_{0.4}Fe_2O_4$ powders

In the samples prepared by physical mixing and one-pot method, exchange coupling interaction between hard ($SrFe_{12}O_{19}$) and soft ($Zn_{0.4}Co_{0.2}Ni_{0.4}Fe_2O_4$) ferrites can be helpful to both align the magnetization and arrange magnetic moments which are parallel to each other. This effect can improve the magnetic properties and get higher saturation magnetization [7]. The magnetic parameters of the composite particles including saturation magnetization M_s, remanent magnetization M_r, coercivity H_c and M_r/M_s ratio obtained from hysteresis loops are shown in Table 3. The high Ms of one-pot composite particles is a consequence of interfacial coupling arising from the alignment of more magnetic moments [27]. If there was no exchange coupling between the two phases, the saturation magnetization of the composite would be:

$$M_s = M_{s,hard} f_{hard} + M_{s,soft} f_{soft} \tag{2}$$

where, $M_{s,hard}$ and $M_{s,soft}$ are the saturation magnetization of hard and soft phase and f_{hard} and f_{soft} are the weight fraction of the hard and soft phase [16]. Due to the fact that M_s of all composite particles are higher than the calculated M_s from equation 2, consequently, in all composite particles prepared via one-pot sol-gel auto combustion and physical mixing methods, there is an exchange coupling between two phases.

Coercivities of all the composite particles are lower than those of the pure hard phase or soft phase for one-pot synthesized composite particles (Fig. 7). This means that by increasing the reverse field, the spinel domain walls move towards the interface between the soft and hard phases and exceed into the hard phase and cause magnetization reverse to that phase. So, the coercivity of the samples decreases in comparison to the hard phase region. At high values of the soft phase (60 and 80 wt.%), the exchange force on the spinel is reduced and the interaction among soft moments becomes important. This reduces the coercivity of composite [28].

Optimum exchange coupling is related to the grain size of the composite particles [2]. Maximum exchange coupling was reached when the critical length of soft

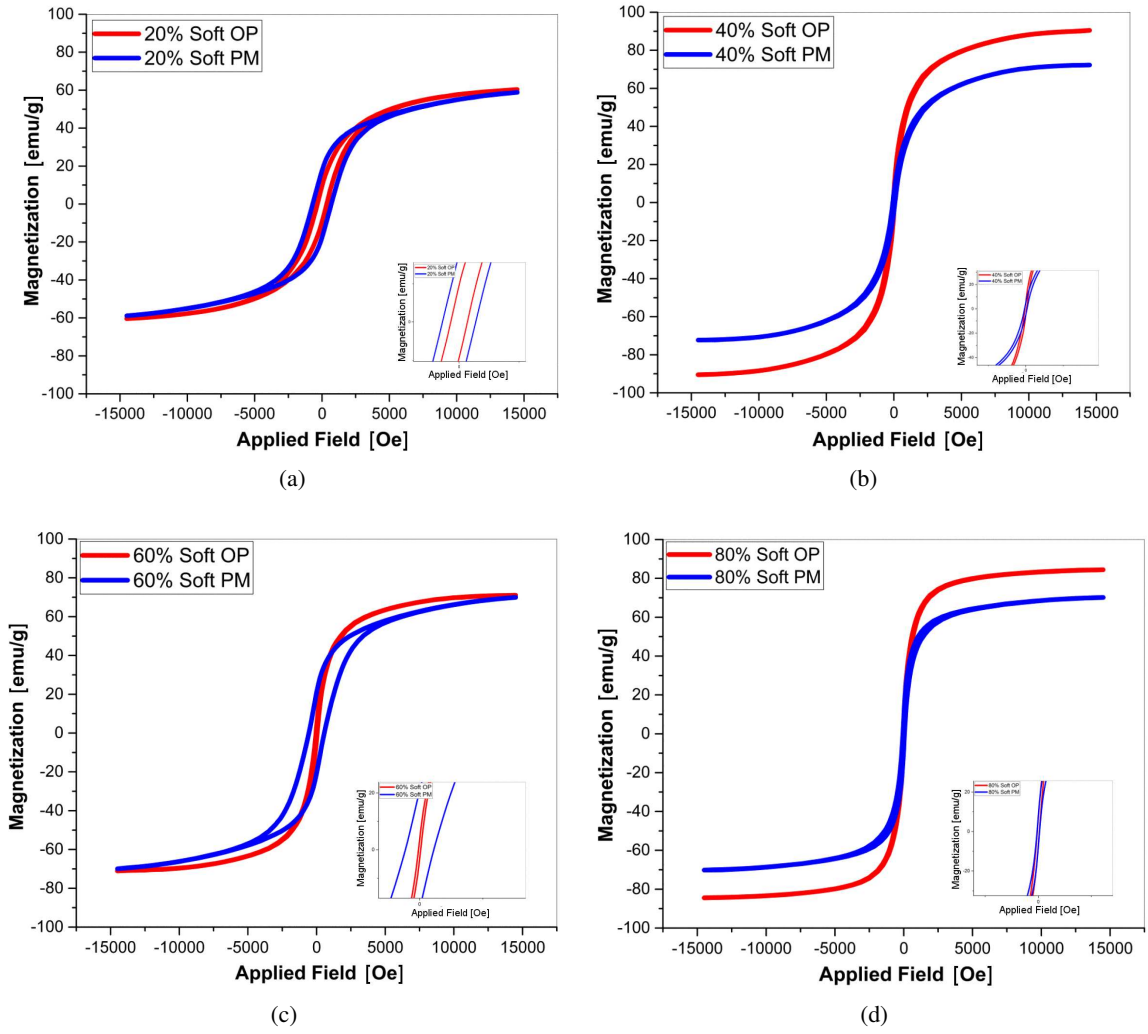

Figure 7. Hysteresis loops of $(SrFe_{12}O_{19})_{1-x}(Zn_{0.4}Co_{0.2}Ni_{0.4}Fe_2O_4)_x$ composite particles prepared by one-pot sol-gel auto-combustion route and physical mixing method with the various amount of soft phase in the composite

Table 3. M_s and H_c values of the $(SrFe_{12}O_{19})_{1-x}(Zn_{0.4}Co_{0.2}Ni_{0.4}Fe_2O_4)_x$ composite particles prepared by one-pot and physical mixing method

Sample	One-pot				Physical mixing				Theoretical M_s without exchange coupling
	H_c [Oe]	M_s [emu/g]	M_r [emu/g]	M_r/M_s	H_c [Oe]	M_s [emu/g]	M_r [emu/g]	M_r/M_s	
Pure soft	64	67	7.5	0.11	–	–	–	–	–
80% soft	50	84	7.2	0.08	60	70	7.2	0.10	63
60% soft	43	71	3.7	0.05	576	69	20	0.28	59
40% soft	54	91	5.5	0.06	90	72	5	0.07	54
20% soft	350	60	9.6	0.16	708	58	17	0.29	50
Pure hard	5818	46	26	0.57	–	–	–	–	–

phase was equal or less than twice of the hard phase domain wall width [10]. The ratio M_r/M_s is reported in Table. 2 to determine the type of intergrain exchanges [29]. For $M_r/M_s = 0.5$ no interaction between particles cause coherent rotations. On the other hand, for $M_r/M_s < 0.5$ magnetostatic interactions cause multi-domain walls existence. Finally, for $M_r/M_s > 0.5$ exchange coupling is present between hard and soft phases. Our results show that the values of M_r/M_s of the composite particles are lower than 0.5, therefore, the particles interact magnetostatically. Thus, the prepared composite particles are good candidates for producing exchange-spring magnets.

IV. Conclusions

Different weight percentages of soft/hard phase $(SrFe_{12}O_{19})_x(Zn_{0.4}Co_{0.2}Ni_{0.4}Fe_2O_4)_{1-x}$ composite particles were prepared with one-pot sol-gel auto-combustion and physical mixing. The FTIR spectra and the XRD patterns confirmed the formation of the desired hard and soft phases. The FESEM micrographs showed

that the hard phase featured a hexagonal platelet-like morphology, while the soft phase was spherical with faceted edges.

The hard/soft ferrite composite particles exhibited good exchange coupling between hard and soft ferrite phases in the samples prepared by physical mixing and one-pot methods and possessed high saturation magnetization. The coercivity of the samples is reduced by increasing soft phase amount, which is related to the dominance of dipolar interaction in soft phase over exchange interaction. Our results show that the values of M_r/M_s of the composite particles are lower than 0.5, therefore; the particles interact magnetostatically. Thus, the prepared composite particles are good candidates for producing exchange-spring magnets.

Acknowledgement: The authors acknowledge the support of Department of Chemistry, Science and Research Branch, Islamic Azad University of Tehran; and are greatly thankful to Shadi Ghezelbash and Sahel Mesdaghi for collaborating in this work.

References

1. S.D. Bader, "Colloquium: Opportunities in nanomagnetism", *Rev. Mod. Phys.*, **78** [1] (2006) 1–15.
2. E.F. Kneller, R. Hawig, "The exchange-spring magnet: a new material principle for permanent magnets", *IEEE Trans. Magn.*, **27** [4] (1991) 3588–3560.
3. S. Hazra, N.N. Ghosh, "Preparation of nanoferrites and their applications", *J. Nanosci. Nanotechnol.*, **14** [2] (2014) 1983–2000.
4. D. Roy, C. Shivakumara, P.S. Anil Kumar, "Observation of the exchange spring behavior in hard-soft-ferrite nanocomposite", *J. Magn. Magn. Mater.*, **321** [5] (2009) L11–L14.
5. D. Roy, P.S.A. Kumar, "Enhancement of $(BH)_{max}$ in a hard-soft-ferrite nanocomposite using exchange spring mechanism", *J. Appl. Phys.*, **106** [7] (2009) 73902.
6. S. Tyagi, H.B. Baskey, R.C. Agarwala, V. Agarwala, T.C. Shami, "Development of hard/soft ferrite nanocomposite for enhanced microwave absorption", *Ceram. Int.*, **37** [7] (2011) 2631–2641.
7. S. Hazra, B.K. Ghosh, M.K. Patra, R.K. Jani, S.R. Vadera, N.N. Ghosh, "A novel 'one-pot' synthetic method for preparation of $(Ni_{0.65}Zn_{0.35}Fe_2O_4)_x$–$(BaFe_{12}O_{19})_{1-x}$ nanocomposites and study of their microwave absorption and magnetic properties", *Powder Technol.*, **279** (2015) 10–17.
8. A. Poorbafrani, H. Salamati, P. Kameli, "Exchange spring behavior in $Co_{0.6}Zn_{0.4}Fe_2O_4$/ $SrFe_{10.5}O_{16.75}$ nanocomposites", *Ceram. Int.*, **41** [1] (2015) 1603–1608.
9. M.A. Radmanesh, S.A. Seyyed Ebrahimi, "Synthesis and magnetic properties of hard/soft $SrFe_{12}O_{19}$/ $Ni_{0.7}Zn_{0.3}Fe_2O_4$ nanocomposite magnets", *J. Magn. Magn. Mater.*, **324** [19] (2012) 3094–3098.
10. S. Torkian, A. Ghasemi, R.S. Razavi, "Magnetic properties of hard-soft $SrFe_{10}Al_2O_{19}$/$Co_{0.8}Ni_{0.2}Fe_2O_4$ ferrite synthesized by one-pot sol-gel auto-combustion", *J. Magn. Magn. Mater.*, **416** (2016) 408–416.
11. X. Shen, F. Song, J. Xiang, M. Liu, Y. Zhu, Y. Wang, "Shape anisotropy, exchange-coupling interaction and microwave absorption of hard/soft nanocomposite ferrite microfibers", *J. Am. Ceram. Soc.*, **95** [12] (2012) 3863–3870.
12. A.R. Ahmad, N.M. Saiden, M.S. Mamat, "Phase distribution and magnetic properties of mechanically alloyed hard/soft ferrite nanocomposites", *J. Supercond. Nov. Magn.*, **30** [11] (2017) 3097–3102.
13. V. Sharma, S. Kumari, B.K. Kuanr, "Exchange-coupled hard-soft ferrites: A new microwave material", *J. Alloys Compd.*, **736** (2018) 266–275.
14. K.P. Remya, D. Prabhu, S. Amirthapandian, C. Viswanathan, N. Ponpandian, "Exchange spring magnetic behavior in $BaFe_{12}O_{19}/Fe_3O_4$ nanocomposites", *J. Magn. Magn. Mater.*, **406** (2016) 233–238.
15. R. Xiong, W. Li, C. Fei, Y. Liu, J. Shi, "Exchange-spring behavior in $BaFe_{12}O_{19}$-$Ni_{0.5}Zn_{0.5}Fe_2O_4$ nanocomposites synthesized by a combustion method", *Ceram. Int.*, **42** [10] (2016) 11913–11917.
16. F. Song, X. Shen, M. Liu, J. Xiang, "Microstructure, magnetic properties and exchange coupling interactions for one-dimensional hard/soft ferrite nanofibers", *J. Solid State Chem.*, **185** (2012) 31–36.
17. K.W. Moon, S.G. Cho, Y.H. Choa, K.H. Kim, J. Kim, "Synthesis and magnetic properties of nano Ba-hexaferrite/NiZn ferrite composites", *Phys. Status Solidi*, **204** [12] (2007) 4141–4144.
18. S. Hazra, M.K. Patra, S.R. Vadera, N.N. Ghosh, "A novel but simple 'one-pot' synthetic route for preparation of $(NiFe_2O_4)_x$-$(BaFe_{12}O_{19})_{1-x}$ composites", *J. Am. Ceram. Soc.*, **95** [1] (2012) 60–63.
19. T. Xie, L. Xu, C. Liu, "Dielectric and magnetic response of Sr-Zn ferrite composite", *RSC Adv.*, **3** [36] (2013) 15856.
20. S.M.A. Radmanesh, S.A. Seyyed Ebrahimi, "Examination the grain size dependence of exchange coupling in oxide-based $SrFe_{12}O_{19}/Ni_{0.7}Zn_{0.3}Fe_2O_4$ nanocomposites", *J. Supercond. Nov. Magn.*, **26** [7] (2013) 2411–2417.
21. T. Xie, L. Xu, C. Liu, "Synthesis and properties of composite magnetic material $SrCo_xFe_{12-x}O_{19}$ (x = 0–0.3)", *Powder Technol.*, **232** (2012) 87–92.
22. M. Grigorova, H.J. Blythe, V. Blaskov, V. Rusanov, V. Petkov, V. Masheva, D. Nihtianova, Ll.M. Martinez, J.S. Muñoz, M. Mikhov, "Magnetic properties and Mössbauer spectra of nanosized $CoFe_2O_4$ powders", *J. Magn. Magn. Mater.*, *183* [1-2] (1998) 163–172.
23. N.W. Gregory, "Elements of X-ray diffraction", *J. Am. Chem. Soc.*, **79** [7] (1957) 1773–1774.
24. A. Ghasemi, S. Ekhlasi, M. Mousavinia, "Effect of Cr and Al substitution cations on the structural and magnetic properties of $Ni_{0.6}Zn_{0.4}Fe_{2-x}Cr_{x/2}Al_{x/2}O_4$ nanoparticles synthesized using the sol-gel auto-combustion method", *J. Magn. Magn. Mater.*, **354** (2014) 136–145.
25. R.W. Gao, W.C. Feng, H.Q. Liu, B. Wang, W. Chen, G.B. Han, P. Zhang, H. Li, "Exchange-coupling interaction, effective anisotropy and coercivity in nanocomposite permanent materials", *J. Appl. Phys.*, **94** [1] (2003) 664–668.
26. T. Schrefl, H. Kronmüller, J. Fidler, "Exchange hardening in nano-structured two-phase permanent magnets", *J. Magn. Magn. Mater.*, **127** [3] (1993) L273–L277.
27. C. Pahwa, S. Mahadevan, S.B. Narang, P. Sharma, "Structural, magnetic and microwave properties of exchange coupled and non-exchange coupled $BaFe_{12}O_{19}/NiFe_2O_4$ nanocomposites", *J. Alloys Compd.*, **725** (2017) 1175–1181.
28. Z.S. Shan, J.P. Liu, V.M. Chakka, H. Zeng, J.S. Jiang, "En-

ergy barrier and magnetic properties of exchange-coupled hard-soft bilayer", *IEEE Trans. Magn.*, **38** [5] (2002) 2907–2909.

29. E.C. Stoner, E.P. Wohlfarth, "A mechanism of magnetic hysteresis in heterogeneous alloys", *IEEE Trans. Magn.*, **27** [4] (1991) 3475–3518.